Cancer cell research 6 (2015) 129-133

www.cancercellresearch.org Article

CT and MRI Diagnosis of Osteolytic Metastases of the Vertebral Column

Xiaonan Cai, Jihua Liu*

Radiology Department, the Affiliated Hospital of Qingdao University, Shandong 266100, China

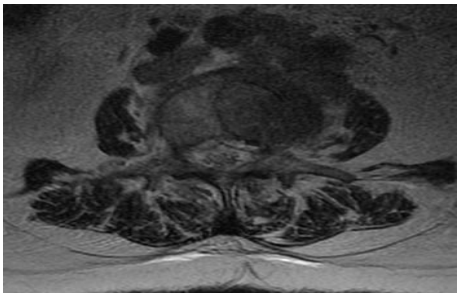

Abstract: **To analyze the CT and MRI features of spinal osteolytic metastases to investigate the diag nostic value of CT and MRI images of this disease. CT and MRI imaging features of 50 patients with spinal osteolytic metastases confirmed pathologically were analyzed retrospectively. CT imaging features: 72 vertebrae were involved in 50 patients, 32 vertebrae showed a rounded soft tissue low density area, 40 vertebrae showed an irregular sheet of soft tissue low density area. Fifty-three of these 72 vertebrae were surrounded with sclerotic margins which were thinner than 2 mm. In 39 vertebrae the cortex was destroyed, while in 11 vertebrae the cortex had expanded into an incomplete crustiform structure. Eight vertebrae were fragmented and appeared as mottling, with imaging showing that the outline of the vertebrae had disappeared, with burst-like bone fragments scattered around, and the vertebrae exhibiting mixed density. Twelve vertebrae were associated with pathologic compression fractures. There were 35 paraspinal soft tissue masses. MRI imaging features: of the 72 osteolytic metastatic vertebrae shown in CT, 62 vertebral lesions showed low signal in T1WI, while T2WI showed a heterogeneous high signal, and T2WI fat-suppressed images also showed a high signal, the 53 vertebrae surrounded by sclerotic margins showed corresponding low signal rings in T1WI. Osteolytic spinal metastases each have their own characteristics in CT and MRI imaging. CT has the ability to make accurate judgments on sclerotic changes in the vertebrae, while MRI is more sensitive to paraspinal soft tissue swelling, soft tissue masses and bone marrow edema. It becomes a specific performance that there ubiquity sclerosis around the lesions. The combination of both CT and MRI can provide accurate and reliable clinical information, and improve the rate of accurate diagnosis.**

Keywords: Spinal; Osteolytic; Metastases; CT; MRI

Received 15 November 2014, Revised 23 December 2014, Accepted 19 January 2014

* Corresponding Author: Yunjie Zeng, zy@qq.com

1. Introduction

The spine is a predilection site for metastases, with approximately 90% of bone metastases being found there[1]. The primary tumors are commonly in the breast, prostate, lung, thyroid gland, gastrointestinal tract, and kidney. Spinal metastases are characterized according to the bone changes and are divided into osteolytic, osteogenic, and mixed, of which osteolytic metastases are the most common. As spiral CT and MRI are widely available, the use of CT and MRI has become an important means of diagnosing spinal metastases. CT and MRI each have their own advantages, and if these two techniques are combined in the process of diagnosis of spinal metastases, diagnostic accuracy can be improved. We retrospectively analyzed CT and MRI image data of 50 patients with osteolytic spinal metastases confirmed by clinical and pathologic findings, focusing on the analysis and comparison of CT and MRI imaging signs in order to improve the level of understanding and diagnosis of the disease.

2. Methods

2.1 General Information

We collected data on 50 cases of osteolytic spine metastases confirmed by pathology and clinical examination in our hospital. The patients comprised 28 males and 22 females, aged 34-82 years, with a mean age of 56.4 years. Among the primary tumors, there were 20 cases of lung cancer, nine cases of breast cancer, eight cases of liver cancer, and one case each of nasopharyngeal carcinoma, cervical cancer, stomach cancer, thyroid cancer, pancreatic cancer, colorectal cancer, and bladder cancer, as well as six cases of thoracolumbar pain with no clear clinical diagnosis. Clinical symptoms and signs: symptoms typically started with localized pain, mostly intermittent at first but later becoming chronic, accompanied by tactile loss and appearance of pathological reflex.

2.2 Examination methods

All patients underwent CT and MRI imaging examinations. CT examination used a GE Light speed 16-slice CT scanner, pitch 1, with a thickness of 2.5-5 mm, distance of 2.5-5 mm. The scan range included the entire vertebral body and attachments. Scanning conditions were 200 mA, 120 KV. MR used a GE Signa 1.5T superconducting magnetic resonance analyzer, with a thickness of 4 mm, distance of 0.5-1 mm, using unenhanced SE T1WI (TR 500–600 ms, TE 10–15 ms), FSE T2WI (TR 3600–4500 ms, TE 80–120 ms), fat suppression FSE T2WI. Image processing was performed on a workstation GE AW 4.2.

3. Results

3.1 Involving site

Three cases involved both the both cervical and thoracic spine, while there were 28 cases of thoracic involvement, nine lumbar cases, seven cases of both thoracic and lumbar involvement, and three cases of both lumbar and sacral involvement. A total of 72 vertebraes were involved, of which a total of 20 attachments were involved in 15 cases, 12 cases involved the canalis spinalis, and there were 35 paraspinal soft tissue masses, 20 paraspinal soft tissue swellings, and 12 pathological compression fractures or accessories fracture (Table 1).

Table 1 Position and number of 50 cases of vertebral invasion

Vertebral invasion	Cervical	Thoracic	Thoracolumbar	Lumbar	Lumbosacral
Case Number	3	28	7	9	3
Percentage	6%	56%	14%	18%	6%

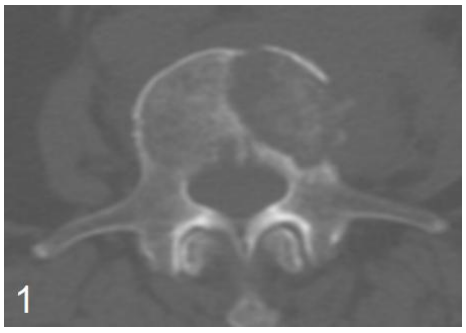

Figure 1. L3 osteolytic vertebral metastases, the edge of the lesion shows a high density calcium signal and the presence of the residual bone shell.

3.2 CT performance

The lesions were visible as soft tissue density bone destruction shadows, with the edge showing mild hardening; the thickness was less than 2 mm, and the lesions were single or multiple, and ranged in size (Figure 1-2). Thirty-two vertebral lesions appeared as round or oval soft tissue density shadows, and 40 vertebral body lesions appeared as irregularly-shaped soft tissue low density shadows. Fifty-three vertebral lesions were associated with bone sclerosis(Figure3A-C), in 39 lesions vertebral cortical bone destruction was evident, in 21 vertebrae the cortex had expanded into an incomplete crustiform structure, while 18 vertebrae were fragmented and were visible as mottling, such that the outline of the vertebrae had disappeared, burst-like bone fragments were scattered around, and the vertebrae were of mixed density (Figure 4A-B). Soft tissue masses could be seen around 35 involved vertebrae, and according to the extent and thickness of the mass, they could be divided into localized and diffuse lesions (Figure5A-B). Of the 14 diffuse lesions, the mass was bigger than ½ the perimeter of the vertebrae at the same level and the maximum thickness was < 2 cm; while of the 21 localized lesions, the mass was less than half the perimeter of the vertebrae at the same level, the mass thickness ranged from 1–7 cm, and six spinal masses were thicker than 6 cm (Table 2).

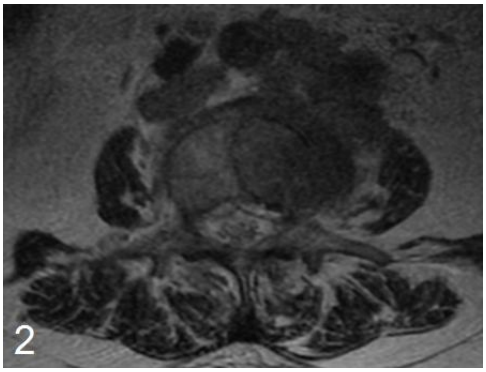

Figure 2. The affected vertebra shows a low signal ring and paraspinal soft tissue mass.

Table 2 The range and size of 35 peripheral soft tissue masses outside the vertebral lesion

Peripheral soft tissue mass	Number of involved vertebrae	Range of the tumor	Thickness of the tumor
Diffuse	14	> ½ perimeter of the vertebrae at the same level	< 2 cm
Localized	21	≤ ½ perimeter of the vertebrae at the same level	1–7 cm

3.3 MR performance

Sixty-two vertebral lesions showed low signal intensity on T1WI, uneven low signal intensity on T2WI, and high signal intensity on a T2WI

fat-suppressed imaging. Ten vertebral lesions showed low signal on T1WI, which was slightly hyperintense on T2WI, and a slightly higher signal on the T2WI fat-suppressed image. According to the vertebral morphology and the number and extent of the lesions within the vertebrae, these 72 vertebraes could be divided into four types. Type I (27 vertebrae): single lesion within the vertebral body, which appeared round or oval, most of the vertebral body was involved, and the boundaries were clear or slightly fuzzy. In this type, 15 lesions involved the lower part of the vertebral spine, and five of them were associated with a slight bulge. Type II (25 vertebrae): multiple nodular lesions in the vertebrae, more distinct boundaries, among the lesions bone marrow signals could be seen, morphology of the vertebra was normal. Type III (eight vertebrae): signals of all vertebrae showed abnormalities, no compression fractures, but two vertebrae exhibited a localized bulge. Type IV (12 vertebrae): signal anomalies associated with compression fractures were observed in most or all of the vertebrae (Figure 6A-C) (Table 3).

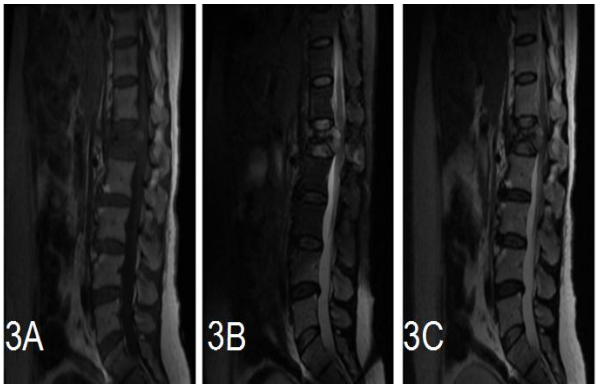

Figure 3. L1 compression fractures, with vertebrae protruding backward and pressing on the dural sac. Lesions show A): a long signal on T1, B): a slightly short signal on T2, and C): a high signal on TDWI.

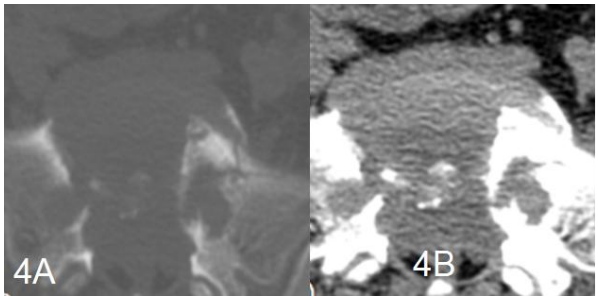

Figure 4. Imaging of vertebra S1 showing bone destruction, in which there are areas of bone sclerosis and high-density calcium(A). The vertebral body has almost entirely been replaced by soft tissue, which shows mixed high and low density, and a paraspinal soft tissue mass can be seen(B).

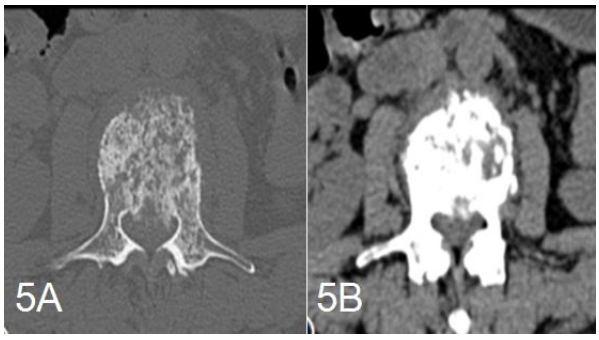

Figure 5. Osteolytic metastases: vertebral lesions were diffuse, the trabecular structure was destroyed, the vertebral boundary was indistinct(A), multiple punctate low density lesions were visible within the vertebra, and the entire vertebra appeared cloudy; such involvement could affect both sides of the attachment(B).

Table 3 Type and lesion characteristics of 72 affected vertebrae.

Type	Number	Characteristics
I	27	Single lesion, round or oval, slightly blurred boundary
II	25	Multiple lesions, normal vertebra morphology, clear boundary
III	8	All vertebrae have signal anomalies, but no compression fractures
IV	12	signal anomalies associated with compression fractures

4. Discussion

The spine is a predilection site for metastases, with the most common type of spinal metastasis being the osteolytic lesion. Habermann *et al.* reported that the incidence of spinal metastases at autopsy was up to 70%, followed by the ribs, skull, femur and pelvis, showing a close relationship with the anatomical structures. The capillary network of red bone marrow is suitable for the growth of tumor emboli, making it a predilection site, and red bone marrow is concentrated in the spine and other elements of the axial skeleton [2]. In addition, the vertebral veins form a separate intravenous line without valves.There is an extensive venous network which is connected to the veins of the breast, kidney, thyroid and prostate, but blood flow is slow, and stagnation or reflux can occur. Metastases can thus invade any part of the

spine, without involving the portal vein, pulmonary vein or superior vena cava system. It has been previously reported [3] that tumors in the spine were mostly distributed in the lumbar region, but in our group of patients tumors were mostly in the thoracic spine, followed by lumbar, cervical and sacral regions, a finding which was the same as the statistical results reported by Meng Qunfei[4]. Osteolytic spinal metastases were located in the rear of the vertebrae, the probable reason for this could be that the vertebral veins are directly connected to the Batson vertebral venous plexus from behind the left vertebrae, other parts of the cancer embolus can then easily reflux into the vertebral venous system through the Batson vertebral venous plexus, and metastatic cells first reach the back of the vertebra and settle there, becoming a common route of spinal metastases [5,6].

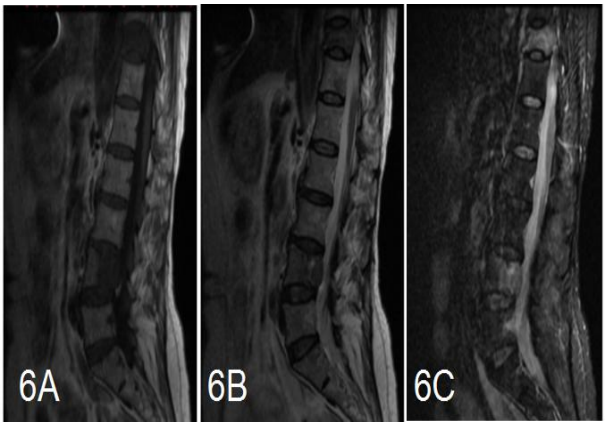

Figure 6. Osteolytic metastases: all or most of the T11, L4 vertebral body was involved, with lesions mainly concentrated in the rear of the vertebra which showed long T1(A) and slightly shorter T2(B) signals, together with high signal in SITR(C). The vertebral body bulged backward and compressed the dural sac, and was accompanied by wedge deformation of the vertebra.

The primary tumor of osteolytic spinal metastases was mostly commonly in organs such as the lung, breast and liver. In this group of 50 cases, the most common primary tumor was lung cancer, accounting for 40% of cases, followed by breast cancer, accounting for 18%, and liver cancer at 16%. The remainders of primary tumors were rare tumors which might be related to the different incidence of malignant tumors between Chinese and other ethnic groups.

The key imaging feature of osteolytic spine metastasis is the destruction of the vertebral bone. Different degrees of hardened edge remain around the lesions, often accompanied by the formation of a paraspinal soft tissue mass. Around the edge of osteolytic spine metastatic lesions different degrees of bone sclerosis can be seen, which appear as a high-density arc calcium shadow on CT and a low signal ring on MR. The edge of some lesions can be seen as low signal rings on MR, but appear indistinct on CT, which might be because of an insufficient degree of calcification of the edge of the lesion. In this group of 72 involved vertebrae from 50 patients, 53 of the vertebrae had a hardened edge, while 19 did not. Of the 53 vertebrae with a hardened edge, the bone sclerosis around the edge of the lesions appeared linear or curved, with a high-density on CT and low signal on MR. The width of the hardened edge ranged from 0.5 to 2.0 mm, and the vertebral lesions were mostly focal lesions, formed as single or multiple lesions with a clearly-defined boundary. Within the lesions the bone destruction was complete. In some cases a little of the bone trabecular structure remained, while in others it was fully replaced by soft tissue, with a diameter of 5 mm to a couple of centimeters. Of the 12 compression fractures, eight vertebrae had a hardened edge around the lesion, and in some cases multiple lesions were integrated with each other, but the borders were clear. In the 19 vertebrae without a hardened edge, the lesions appeared diffuse, and mainly involved bone marrow infiltration, with relatively minor damage to the trabeculae. Lesions were visible as areas with sparse and indistinct trabecular structure; the boundary edge of the lesion was unclear, the typical lesion had a "pepper and salt" appearance of punctate hypodense regions with a diameter of less than 3 mm distributed throughout the vertebra. These lesions could affect both sides of the attachment, and in four vertebrae were associated with compression fractures, which can be easily misdiagnosed in the early period.

5. Differential diagnosis

Differential diagnosis of spinal metastases is difficult, because varying degrees of different types may produce similar symptoms to various bone tumors [7]. If there is a history of primary malignancy, unexplained back pain and progression, and CT and MRI show spinal bone destruction, the diagnosis can be confirmed [8]; however if there is no primary malignancy, it needs to be distinguished mainly from the following possibilities.

5.1 Myeloma

Single or multiple myeloma can be confused with single or multiple vertebral osteolytic metastases; they all have a similar age of onset, and the bone destruction does not involve the intervertebral discs, while pathological vertebral fractures can occur in both cases. The key points of identification are as follows: myeloma is mainly diagnosed on the basis of osteoporosis and is associated with bone destruction with a clear boundary. The attachment is rarely involved and soft tissue masses are rarely present, while metastases are often larger. A key finding is that Bence Jones protein is positive in diagnosis of myeloma.

5.2 Spinal tuberculosis

Most patients with spinal tuberculosis have a history of tuberculosis. The lesions are mostly located in the central anterior, rarely involving attachments, but always involving the adjacent intervertebral disc, and there are localized or diffuse swellings in the soft tissue beside the vertebrae, abscesses beside the vertebrae and soft tissue calcification. There is no obvious strengthening on CT enhanced scans, or strengthening is only present in the margins of vertebral abscesses. Patients with osteolytic metastases mainly have a primary lesion, the tumor mostly infringes the back of the vertebrae and the bony structure of the attachments, the lesions can be jumping, with dead bone seldom seen, rarely involve the intervertebral disc and generally spread along the front longitudinal, but they can spread around and form a vertebral side tissue mass containing a few calcifications, which are obviously strengthened in a CT enhanced scan.

5.3 Differential diagnosis of pathological fracture

Fractures mainly need to be distinguished from compressibility fractures caused by osteoporosis, which are more commonly seen in older postmenopausal women who have widespread osteoporosis. Osteoporotic compressibility fractures appear concave on the edge of the vertebra like a fish ridge, the intervertebral disc appears relatively widened as a result of double-convex deformation, while the vertebrae become double-concave, there is no spinal canal stenosis, and no soft tissue masses beside the vertebrae. In contrast, compressibility fractures caused by osteolytic metastases have bone defects, and lesions can involve the posterior wall of the vertebral pedicle, leading to spinal stenosis, while soft tissue masses can be seen beside the vertebrae.

6. Conclusion

CT can clearly show the changes of trabecular, cortical and periosteal bone, and the calcification and ossification of the edge of the lesion. MRI can clearly show the scope of the tumor, changes of the paraspinal soft tissue and edema of the bone marrow. Combining both CT and MRI imaging features provides accurate and reliable information for the clinical diagnosis of spinal osteolytic metastases.

References

[1] Zhang FZ, Liu L. The value of CT and MRI in the diagnosis of spinal metastases. Practical Journal of Medicine Imaging，12(4): 2011 235-237.

[2] Kricun ME. Red-yellow marrow conversion: its effect on the location of some solitary bone lesions. Skelet Radiol，14(1): 1985 10-19.

[3] Algra PR, Heimans JJ, Valk J. Do metastasis invertebrae begin in the body or the pedicle Imaging study in 45 patients. AJR, 158(6): 1992 1275-1279.

[4] Meng QF, Jiang B, Chen YM. CT study of vertebral metastasis: re-realization of the diagnostic role of the vertebral pedicle sign. Chinese Journal of Radiology magazine, 34(8): 2000 518-522.

[5] Lo LD, SchWeitzer ME, Juneja V. Are 15 fractures an indicator of metastasis? Skeletal Radiology, 29: 2000 454-458.

[6] Epstein Bs, ed. Spine x-ray diagnostics. Duan CX, Interpret. 1st edition. Shanghai: Shanghai Science and Technology Press: 1987 136-139.

[7] Zheng SS, Gao B, liu B. CT diagnosis and clinical. Hefei: Anhui Science and Technology Press: 2011 731.

[8] Liang FM, Yin HZ. Comparison of radiographic lumbar disease. Jinan: Shandong Science and Technology Press: 2005 212-214.